Facile Synthesis, Geometry, and 2′-Substituent-Dependent in Vivo Activity of 5′-(E)- and 5′-(Z)-Vinylphosphonate-Modified siRNA Conjugates

Rubina Giare Parmar,[†] Christopher R. Brown,[†] Shigeo Matsuda,[†] Jennifer L. S. Willoughby,[†] Christopher S. Theile,[†] Klaus Charissé,[†] Donald J. Foster,[†] Ivan Zlatev,[†] Vasant Jadhav,[†] Martin A. Maier,[†] Martin Egli,[‡] Muthiah Manoharan,*,[†] and Kallanthottathil G. Rajeev*,[†]

[†]Alnylam Pharmaceuticals, 300 Third Street, Cambridge, Massachusetts 02142, United States

[‡]Department of Biochemistry and Center for Structural Biology, Vanderbilt University, School of Medicine, Nashville, Tennessee 37232, United States

Ⓢ *Supporting Information*

ABSTRACT: (E)-Vinylphosphonate ((E)-VP), a metabolically stable phosphate mimic at the 5′-end of the antisense strand, enhances the in vivo potency of siRNA. Here we describe a straightforward synthetic approach to incorporate a nucleotide carrying a vinylphosphonate (VP) moiety at the 5′-end of oligonucleotides under standard solid-phase synthesis and deprotection conditions by utilizing pivaloyloxymethyl (POM) protected VP-nucleoside phosphoramidites. The POM protection enhances scope and scalability of 5′-VP-modified oligonucleotides and, in a broader sense, the synthesis of oligonucleotides modified with phosphonate moieties. Trivalent N-acetylgalactosamine-conjugated small interfering RNA (GalNAc-siRNA) comprising (E)-geometrical isomer of VP showed improved RISC loading with robust RNAi-mediated gene silencing in mice compared to the corresponding (Z)-isomer despite similar tissue accumulation. We also obtained structural insights into why bulkier 2′-ribosugar substitutions such as 2′-O-[2-(methylamino)-2-oxoethyl] are well tolerated only when combined with 5′-(E)-VP.
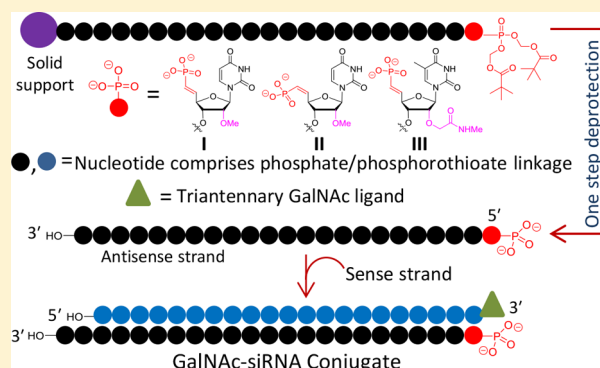
■ INTRODUCTION

In recent years, a number of investigational RNA interference (RNAi) based therapeutics have advanced into clinical studies, bringing the field closer to the realization of the immense potential of this approach toward unmet medical needs.[1−6] Most recently, positive results from APOLLO phase 3 trial of patisiran,[7] an investigational RNAi therapeutic being developed for patients with hereditary ATTR (hATTR) amyloidosis with polyneuropathy,[8,9] are paving the way for RNAi therapeutics to become a reality for patients.[10,11] Another important breakthrough in the field was accomplished with the development of targeted delivery utilizing a synthetic trivalent N-acetylgalactosamine (GalNAc) ligand that is covalently conjugated to a chemically modified small interfering RNA (siRNA).[12] This strategy enables safe and effective targeted delivery of siRNA to the liver mediated by the asialoglycoprotein receptor (ASGPR) located on the surface of hepatocytes,[13−15] which triggers clathrin-mediated endocytosis to enable intracellular delivery of siRNA to elicit RNAi-mediated RNA silencing, depicted in Figure 1. Chemical modifications on the GalNAc-siRNA conjugates[12] are necessary for metabolic stability but can significantly impair the activity of Clp1 kinase,[16] believed to facilitate 5′-end phosphorylation of the antisense (or guide)

strand, a requirement for efficient loading into the Argonaute 2 (Ago2) protein,[17,18] the key component of the RNA-induced silencing complex (RISC). Incorporation of a natural 5′-monophosphate (5′-P) into GalNAc-siRNA conjugates has been found to be ineffective due to rapid dephosphorylation by lysosomal acid phosphatases, after entry into the endocytic pathway.[19] To circumvent this issue, we and others have recently utilized metabolically stable 5′-(E)-vinylphosphonate (5′-(E)-VP),[19−23] a phosphate mimic, to enhance RISC loading and RNAi activity of GalNAc-siRNA conjugates. The structural similarity of 5′-(E)-VP to 5′-P supports successful RISC loading of the antisense strand carrying 5′-(E)-VP. Recently two independent crystal structure studies[24,25] of Ago2-loaded antisense strand modified with 5′-(E)-VP have elucidated how the 5′-nucleotide binding pocket in the MID and PIWI subdomains of human Ago2 is able to adjust key residues to compensate for and accommodate the structural perturbation exerted by the 5′-(E)-VP moiety in place of the natural 5′-P.

These structural findings encouraged us to further explore the potential of 5′-(E)-VP as a 5′-monophosphate mimic in
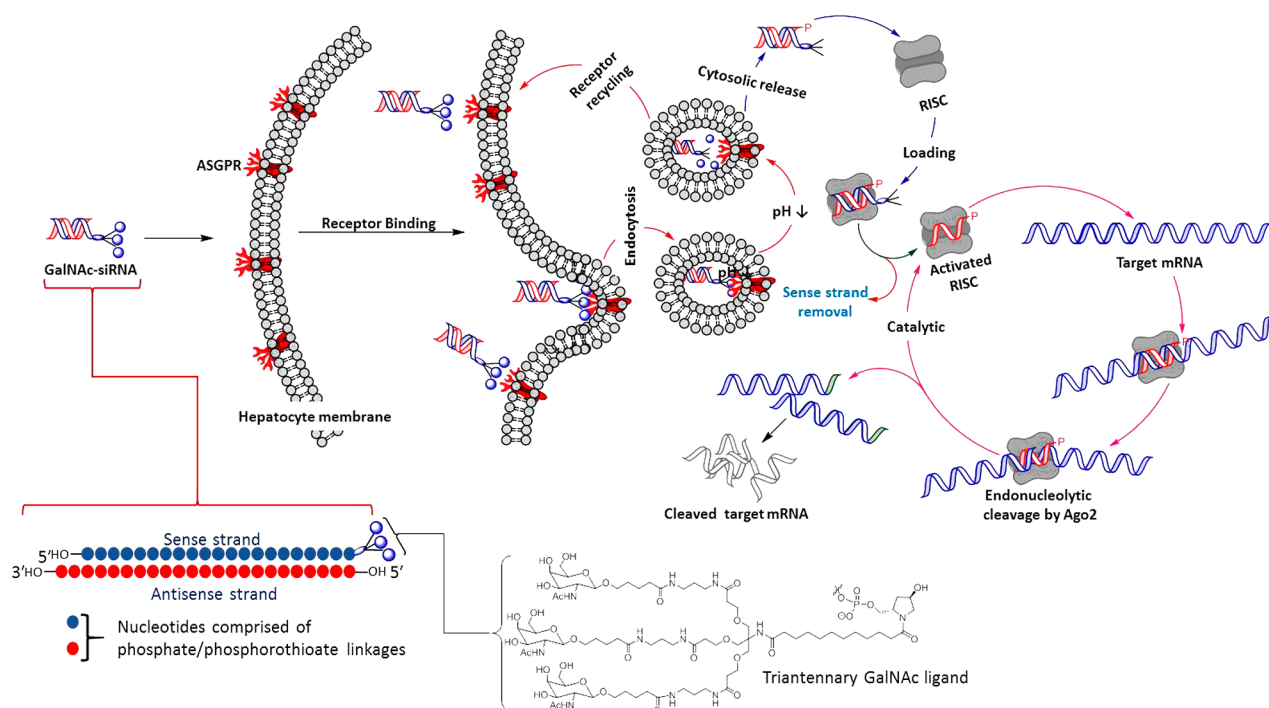
Figure 1. Schematic of ASGPR-mediated endocytosis of GalNAc-siRNA conjugate into hepatocytes for intracellular delivery leading to RNAi-mediated silencing of target mRNA. After internalization of the conjugate by ASGPR, the low pH of the early endosomes results in detachment of the GalNAc-siRNA from the receptor[13] with concomitant cleavage of the anomeric linkage of the GalNAc moiety from the conjugate.[29] A fraction of the siRNAs from the endosome escape into the cytosol to engage with RISC to form antisense strand-loaded functional RISC, for which endogenous phosphorylation at the 5′-end of the antisense strand by kinases is a prerequisite, which then finds its target mRNA to produce endonucleolytic cleavage by RISC-associated Ago2 endonuclease. After product release, activated RISC engages with new mRNA molecules in a catalytic manner.[30]
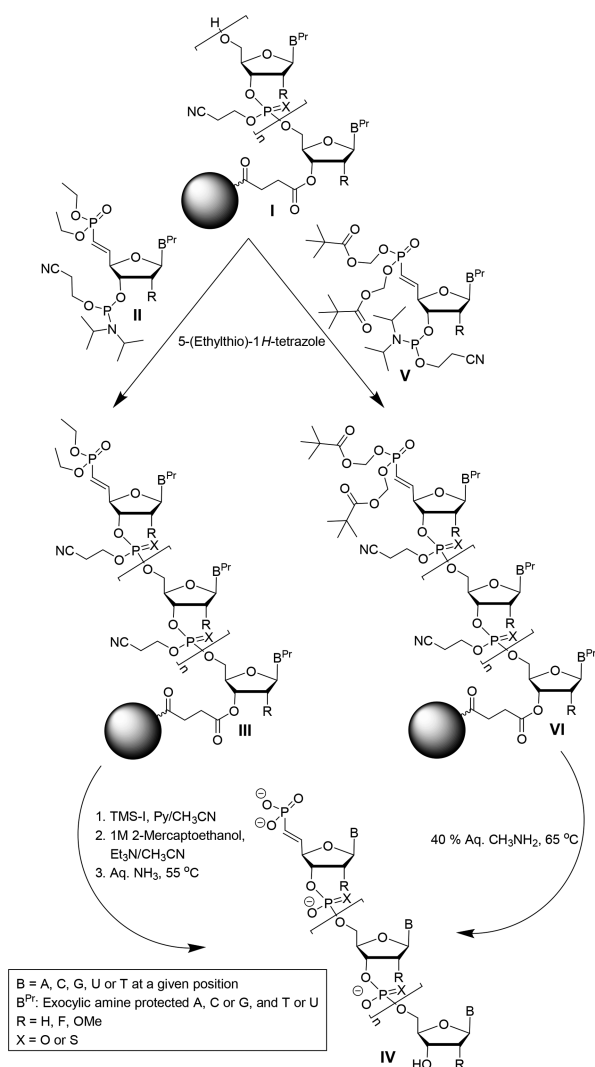
combination with a 2′-modified ribonucleotide at the 5′-end of the antisense strand. However, the synthetic limitation while introducing the VP moiety to the 5′-end of an oligonucleotide using the reported procedure[20,21] prompted us to explore an alternative method compatible with standard solid-phase synthesis, which could enable large scale synthesis of 5′-phosphonate-modified oligonucleotides. The pivaloyloxymethyl (POM) group has also been used for 2′-hydroxyl protection during solid-phase synthesis of oligoribonucleotides, where the protecting group was removed under single-step aqueous ammonia deprotection conditions.[26] In addition, the bis-(pivaloyloxymethyl) protection on nucleoside phosphonates has been widely used for the nucleotide prodrug approach.[27,28] In the present work we report efficient use of POM protection for introducing a VP moiety at the 5′-end of the antisense strand under standard solid phase synthesis and deprotection conditions (Scheme 1, method B). Also reported are (i) comparison of RNAi-mediated gene silencing activity of E- and Z-isomers of VP at the 5′-end of the antisense strand, in vitro and in vivo in mice, (ii) Ago2-loading efficiency of the geometrical isomers, and (iii) impact of the moderately bulky 2′-substituent 2′-O-[2-(methylamino)-2-oxoethyl] (2′-O-NMA) on the 5′-terminal nucleotide of the antisense strand in the presence and absence of 5′-(E)-VP on siRNA activity.

■ RESULTS AND DISCUSSION

The GalNAc-siRNA conjugates containing a 5′-(E)-VP moiety utilized in previous studies were synthesized using the corresponding phosphoramidite with diethyl-protected trans-vinylphosphonate[21] **II** (Scheme 1, method A). Deprotection of the solid support-bound oligonucleotide **III** carrying the
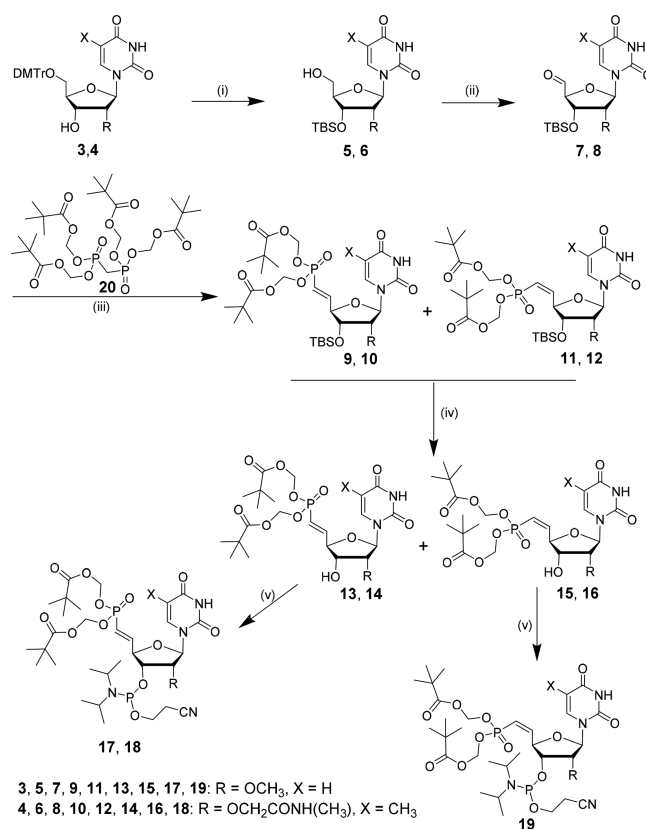
diethyl-protected VP moiety requires additional reagents and steps that are not used during conventional oligonucleotide synthesis. These include treatment of the oligonucleotide on the support with iodotrimethylsilane in pyridine/acetonitrile under anhydrous conditions for 0.5 h for selective removal of the ethyl moieties from the protected phosphonate, followed by quenching of the reaction mixture with 1 M 2-mercaptoethanol in a 1:1 mixture of triethylamine and acetonitrile. After the phosphonate deprotection, the support-bound oligonucleotide is subjected to concentrated aqueous ammonia treatment either at 55 °C for 6 h or at room temperature for 16 h to obtain the fully deprotected oligonucleotide **IV**. The coupling of nucleoside phosphoramidite **V** modified with POM-protected VP to the 5′-end of a growing oligonucleotide **I** on solid support affords support-bound POM-protected VP-containing oligonucleotide **VI** that can be fully deprotected in one step under conventional oligonucleotide deprotection conditions using aqueous methylamine to yield the oligonucleotide **IV** (Scheme 1, method B).

The fully protected 5′-(E)-VP **17** and **18** and 5′-(Z)-VP **19** phosphoramidites for incorporation into siRNA were synthesized from their corresponding nucleoside precursors 3[31] and 4[32] as shown in Scheme 2. Treatment of the 5′-O-DMTr-protected nucleosides **3** and **4** with TBS-Cl in the presence of imidazole in DMF followed by treatment with trifluoroacetic acid in dichloromethane at ambient temperature afforded the corresponding 3′-O-TBS protected nucleosides **5** and **6**. Oxidation of the 5′-hydroxyl group of **5** and **6** using Dess–Martin periodinane in dichloromethane at 0 °C afforded the corresponding aldehydes **7** and **8**, respectively.[33] The mixture of 5′-(E)- and 5′-(Z)-bis(pivaloyloxymethyl)-phosphonates **9** and **11** with (E) to (Z) ratio of about 9:1 (based on ^{1}H NMR)

Scheme 1. Synthesis of Oligonucleotide Containing 5'-(E)-Vinylphosphonate Modification

Scheme 2. Syntheses of POM-Protected 5'-(E)- and 5'-(Z)-VP 3'-Phosphoramidite Monomers[a]

3, 5, 7, 9, 11, 13, 15, 17, 19: R = OCH$_3$, X = H
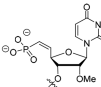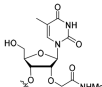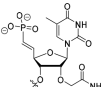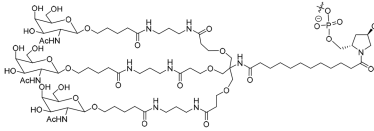4, 6, 8, 10, 12, 14, 16, 18: R = OCH$_2$CONH(CH$_3$), X = CH$_3$

[a](i) a) TBS-Cl, imidazole/DMF, rt, 17 h; (b) CF$_3$COOH/CH$_2$Cl$_2$, rt, 2 h; (ii) Dess−Martin periodinane, CH$_2$Cl$_2$, yield = 70%; (iii) NaH/THF, −78 °C, yield = 72%, mixture of E and Z isomers; (iv) HCOOH/H$_2$O (1:1), 24 h; separation of E and Z isomers (v) 2-cyanoethyl N,N,N',N'-tetraisopropylphosphorodiamidite, 5-ethylthio-2H-tetrazole/acetonitrile.

and a combined yield of 72% was prepared from the aldehyde **7** and tetrakis[(pivaloyloxy)methyl] methylenediphosphonate[34] (**20**) by following a modified Horner−Wadsworth−Emmons (HWE) olefination.[35] Attempts to separate the two geometric isomers **9** and **11** by normal silica gel or by reverse phase HPLC (RP-HPLC) were unsuccessful. Treatment of the isomeric mixture with 1:1 formic acid and water afforded the desilylated mixture **13** and **15** in quantitative yield. The (E)- and (Z)-isomer **13** and **15**, with isolated yields of 55% and 9%, respectively, were separated at this stage using flash column chromatography followed by RP-HPLC as described in the Supporting Information. Phosphitylation[36] of the isolated **13** and **15** afforded the corresponding phosphoramidites **17** and **19**, respectively. Compounds **14** and **16** and the phosphor-amidite **18** bearing a 2'-O-NMA moiety were prepared from the aldehyde **8** in a similar way as described above.

The ^{31}P NMR chemical shift of the (E)-isomer **13** (δ 18.14 ppm) showed a distinct 2.3 ppm downfield shift compared to the (Z)-isomer **15** (δ 15.85 ppm) in DMSO-d_6; see Supporting Information Figure S6 for comparison of chemical shifts. The (E)-isomer **14** (δ 17.05 ppm) showed a similar deshielding compared to the corresponding (Z)-isomer **16** (δ 14.70 ppm) in DMSO-d_6. The (E)-vinyl protons of both compounds **13**

and **14** showed a slight downfield shift compared to the corresponding (Z)-vinyl protons, respectively (Supporting Information, Figure S9).

Oligonucleotide synthesis was performed on a DNA/RNA synthesizer. Each POM-protected VP monomer shown in Scheme 2 was coupled to the 5'-end of the solid-support-bound and DMTr-unprotected oligonucleotide **I** under the standard solid-phase synthesis conditions as reported (Scheme 1).[37] The POM-protected VP-containing oligonucleotides were then treated with 40% aqueous methylamine solution for 15 min at 65 °C to obtain the fully deprotected oligonucleotides in one step. The crude oligonucleotides were purified by anion-exchange HPLC, and the integrity of each oligonucleotide was confirmed by analytical IEX-HPLC and by LC−MS analyses (Table S1). The siRNAs in Table 1 were prepared from the corresponding sense and antisense strands as reported and were analyzed for purity, endotoxin, and osmolality prior to evaluation.[12]

To study the effect of 5'-(E)- and 5'-(Z)-VP-modified GalNAc-siRNA conjugates on RNAi-mediated gene silencing, siRNAs targeting two different genes in the liver, transthyretin (Ttr)[12] and apolipoprotein B (ApoB),[38] were evaluated in vitro and in vivo in mice. The siRNAs used in this study were fully chemically modified as previously reported,[12] differing only at

Table 1. GalNAc-siRNA Conjugates Used in This Study

Target	Sense/Antisense (5′-3′)[a]	siRNA	X =
Ttr	5′-*A*•a•*CaGuGuUCUuGcUcUaUaA*-L/ 5′-**X**•*U*•a*UaGaGcA*aga*AcAcUgUu*•u•u	**1**	u
		1E-VP	5′-(*E*)-VPu
		1Z-VP	5′-(*Z*)-VPu
ApoB	5′-*C*•c•*UgGaCaUUCaGaAcAaGaA*-L/ 5′-**X**•*U*•c*UuGuUcU*gaa*UgUcCaG*g•g•u	**2**	u
		2E-VP	5′-(*E*)-VPu
		2Z-VP	5′-(*Z*)-VPu
		2$_{NMA}$	NMA-T
		2E-VP$_{NMA}$	5′-(*E*)-VP$_{NMA}$T

5′-(*E*)-VPu   5′-(*Z*)-VPu   NMA-T

5′-(*E*)-VP$_{NMA}$T   L

[a]Italicized upper case and normal lower case letters indicate 2′-deoxy-2′-fluoro (2′-F) and 2′-*O*-methyl (2′-OMe) sugar modifications, respectively, to adenosine (A), cytidine (C), guanosine (G), and uridine (U), and • indicates a phosphorothioate (PS) linkage.

Table 2. In Vitro Potency As Measured by Half-Maximal Inhibitory Concentration (IC$_{50}$) of Modified GalNAc-siRNA Conjugates after Transfection into Primary Mouse Hepatocytes[a]

				conjugate				
	1	**1E-VP**	**1Z-VP**	**2**	**2E-VP**	**2Z-VP**	**2**$_{NMA}$	**2E-VP**$_{NMA}$
IC$_{50}$ (nM)	0.06	0.035	0.153	7.231	0.978	>10.0	2.024	0.131

[a]See Supporting Information, Figure S1, for IC$_{50}$ curves.
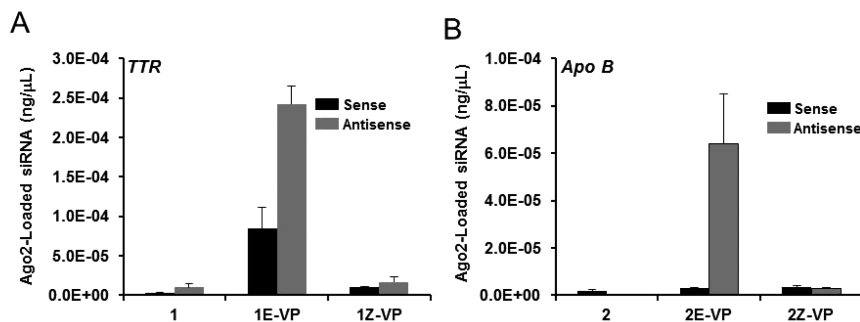
Figure 2. Impact of 5′-(*E*)-VP and 5′-(*Z*)-VP on in vitro Ago2 loading of GalNAc-siRNA conjugates targeting (A) *Ttr* and (B) *ApoB*. Error bars represent standard error.

the 5′-end of the antisense strand with 5′-OH, 5′-(*E*)-VP, or 5′-(*Z*)-VP (Table 1).

The in vitro activity of GalNAc-siRNA conjugates was evaluated in primary mouse hepatocytes under transfection conditions. Conjugate **1E-VP** targeting *Ttr* showed improved potency over parent conjugate **1**, whereas conjugate **1Z-VP** showed diminished in vitro activity (Table 2). This trend was

even more pronounced in the second set of GalNAc-siRNA conjugates targeting *ApoB* with the in vitro potency in the order of **2E-VP** > **2** > **2Z-VP**. More strikingly, the potency improvement for VP-modified siRNA, **2E-VP**$_{NMA}$, that contains 2′-*O*-[2-(methylamino)-2-oxoethyl]ribosugar (2′-*O*-(*N*-methyl-acetamido, 2′-*O*-NMA)[32] modification at position 1 on the antisense strand was 15-fold over its parent siRNA **2**$_{NMA}$.
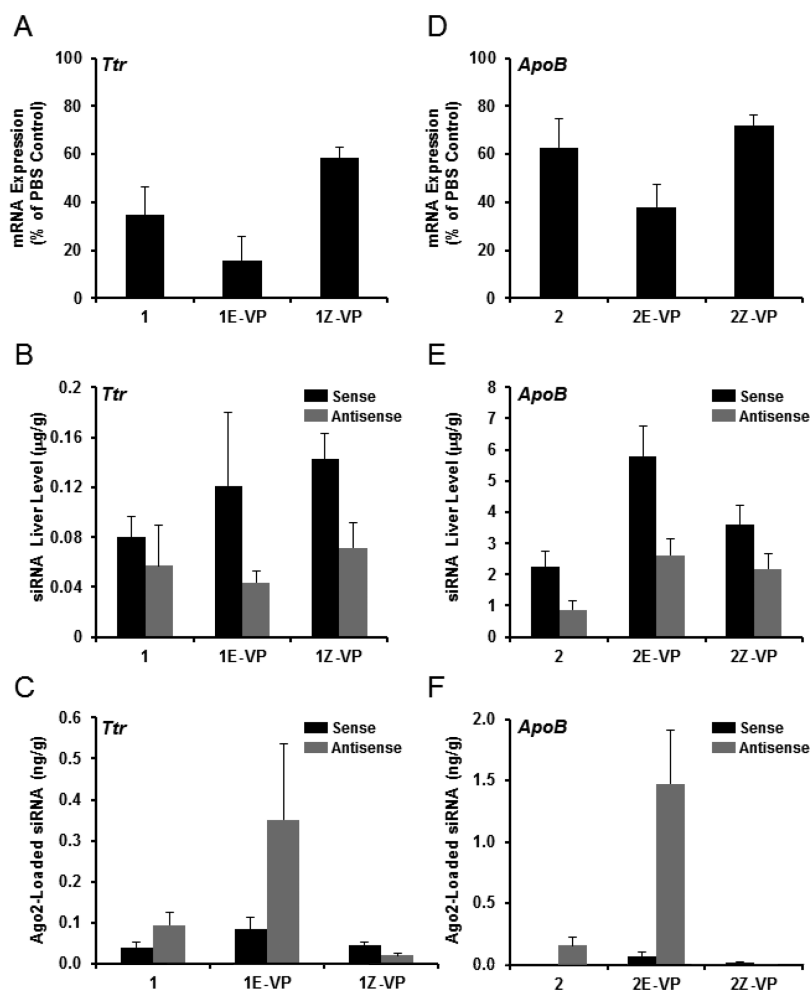
Figure 3. RNAi-mediated gene silencing in mouse by GalNAc-siRNA conjugates: (A) **1**, **1E-VP**, and **1Z-VP** targeting *Ttr* and (D) **2**, **2E-VP**, and **2Z-VP** targeting *ApoB* at day 7 postdose after a single subcutaneous dose of 1 mg/kg for *Ttr* and 10 mg/kg for *ApoB*, n = 3. Total liver exposure of conjugates targeting the genes: (B) *Ttr* and: (E) *ApoB*. Ago2 loading of conjugates targeting: (C) *Ttr* and: (F) *ApoB*. Error bars represent standard error. See Supporting Information, Figure S2, for the corresponding individual animal data.

To correlate the potency with RISC loading, the siRNA conjugates were evaluated in vitro using cell lysates containing overexpressed FLAG-HA-tagged human Ago2. In agreement with its observed in vitro potency (Table 2), the *Ttr*-targeting conjugate **1E-VP** showed higher Ago2 loading than parent conjugate **1**, whereas loading of **1Z-VP** was comparable to parent (Figure 2A). A similar trend was observed with *ApoB*-targeting conjugates (Figure 2B). Parent conjugate **2** was barely detectable in the assay, whereas conjugate **2E-VP** showed a substantial increase in Ago2 loading. The loading of **2Z-VP** was slightly higher than parent but significantly lower than **2E-VP**. Collectively, these results corroborate our in vitro transfection data (Table 2) and suggest that the increase in conjugate potency observed with (*E*)-VP conjugates arises from the increased loading onto Ago2.

To investigate whether the improved in vitro potency would translate in vivo, all GalNAc-siRNA conjugates (**1**, **1E-VP**, **1Z-VP**, **2**, **2E-VP**, and **2Z-VP**, Table 1) were evaluated in mice. On the basis of the in vivo efficacy of the parent conjugate, GalNAc-siRNA conjugates targeting *Ttr* (**1**, **1E-VP**, **1Z-VP**) and *ApoB* (**2**, **2E-VP**, **2Z-VP**) were subcutaneously dosed at 1 and 10 mg/kg, respectively. At day 7 postdose, conjugate **1E-VP** showed remarkable improvement in liver *Ttr* mRNA reduction (∼85%) compared to parent conjugate **1** (∼64%)

(Figure 3A). In vivo data of **1E-VP** conjugate in mice reported earlier[25] were then compared with the corresponding **1Z-VP** conjugate. **1Z-VP**-mediated *Ttr* mRNA reduction (∼40%) was inferior to that shown by the parent conjugate (∼64%). To further investigate the effect of **1E-VP** and **1Z-VP**, total liver and Ago2-loaded levels of the sense and antisense strands for each GalNAc-siRNA conjugate were quantified as previously described.[25] While total siRNA liver levels for conjugates **1**, **1E-VP**, and **1Z-VP** were similar (Figure 3B), a ∼5-fold increase in antisense strand loading into Ago2 was observed with the **1E-VP** conjugate compared to parent conjugate **1** (Figure 3C). In contrast, the levels of RISC-loaded antisense strand of **1Z-VP** were lower than that of parent, in good agreement with the inferior silencing activity.

A similar trend was observed for conjugates targeting *ApoB* (**2**, **2E-VP**, and **2Z-VP**, Table 1). At day 7 postdose, conjugate **2E-VP** showed improved *ApoB* mRNA reduction (∼62%) as compared to parent conjugate **2** (∼37%), whereas **2Z-VP** showed only a 28% reduction (Figure 3D). Total siRNA liver levels were higher for both **2E-VP** and **2Z-VP** compared to the parent (Figure 3E). This may be a consequence of the previously proposed enhancement in metabolic stability against exonucleases provided by the VP modification at the 5′ end of the antisense strand.[19] Conjugate **2E-VP** showed an ∼9-fold
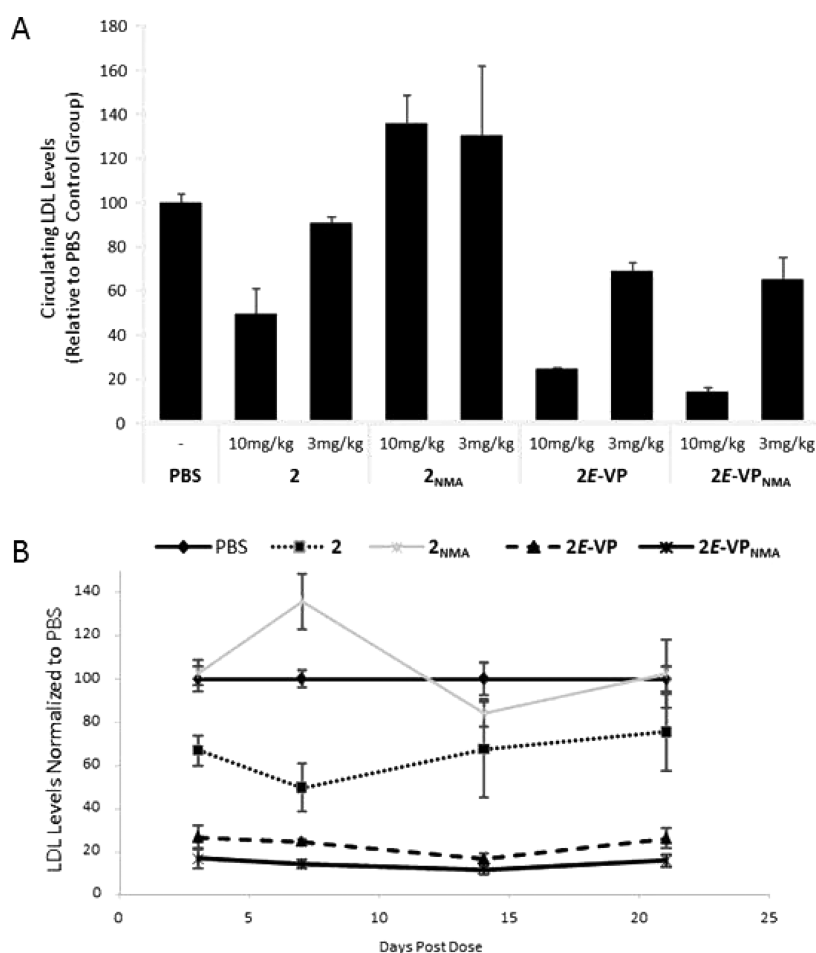
Figure 4. (A) LDL levels assayed 7 days following a single 3 or 10 mg/kg subcutaneous dose of siRNA conjugates **2**, **2**$_{NMA}$, **2E-VP**, and **2E-VP**$_{NMA}$ targeting the *ApoB* gene in liver. (B) LDL levels at days 3, 7, 14, and 21 after a 10 mg/kg subcutaenous dose of conjugates **2**, **2**$_{NMA}$, **2E-VP**, and **2E-VP**$_{NMA}$. LDL levels were normalized to the PBS control group for each time point, *n* = 3 per group; error bars represent standard error. See Supporting Information, Figure S3, for the corresponding individual animal data.

improvement in antisense strand loading onto Ago2 over the parent conjugate **2** (Figure 3F). However, no improvement was observed with conjugate **2Z-VP**. Taken together, these results suggest that the improved in vivo activity observed with both 5′-(*E*)-VP conjugates targeting *Ttr* and *ApoB* was due to increased RISC loading of the modified antisense strands. The poor in vivo RISC-loading of the 5′-(*Z*)-VP-modified siRNAs confirm, as reported,[21] that the *cis*-vinylphosphonate isomer is not a good 5′-monophosphate mimic and does not support enhanced Ago2 binding despite increased liver accumulation compared to their corresponding parent conjugates.

We further evaluated the impact of 2′-ribosugar modification of 5′-(*E*)-VP containing nucleotide on in vivo efficacy and duration of gene silencing in mice. The 2′-*O*-NMA modification in oligonucleotides has shown excellent binding affinity to complementary RNA due to its C3′-*endo* conformation, extended gauche interactions, and enhanced nuclease stability.[39] We envisioned that the RNA-affinity enhancing 2′-*O*-NMA ribosugar at the N1 position of the antisense strand in combination with 5′-(*E*)-VP would provide useful insight into the effect of moderately bulky substitutions at the 2′-position on RISC loading and hence RNAi activity of siRNA. The RNAi-mediated gene silencing activity of siRNAs containing 2′-modified nucleotides 5′-(*E*)-VPu and 5′-(*E*)-VP$_{NMA}$T were compared after incorporating the VP-modified

nucleosides at the 5′-end of antisense strands using the corresponding 3′-phosphoramidite monomers **17** and **18** (Scheme 1, Table 1).

The GalNAc-siRNA conjugates **2**, **2**$_{NMA}$, **2E-VP**, and **2E-VP**$_{NMA}$ (Table 1) targeting *ApoB* were evaluated in mice at 3 or 10 mg/kg dose levels utilizing LDL as a serum biomarker to monitor conjugate activity.[38] Both **2E-VP** and **2E-VP**$_{NMA}$ showed superior target reduction over their parent conjugates **2** and **2**$_{NMA}$, respectively (Figure 4A). Interestingly, parent conjugate **2**$_{NMA}$ did not show any activity at either dose, suggesting that the moderately bulky 2′-*O*-NMA may be even less compatible for endogenous phosphorylation than 2′-*O*-methyl. The combination of 2′-*O*-NMA with the phosphate mimic 5′-(*E*)-VP (conjugate **2E-VP**$_{NMA}$), on the other hand, not only restored but enhanced gene silencing to the same level as that of the **2E-VP** conjugate indicating that the additional steric bulk at the 2′-position does not prevent RISC loading. Further, animals that received a 10 mg/kg dose of either **2E-VP** or **2E-VP**$_{NMA}$ showed robust and sustained LDL lowering 21 days after dosing (Figure 4B), whereas LDL levels in animals that received the control siRNAs were back to baseline 14 days postdose. No noticeable difference in efficacy and duration of activity was observed between the siRNAs **2E-VP** and **2E-VP**$_{NMA}$ within the evaluation period. The effect of the enhanced

metabolic stability of **2E-VP$_{NMA}$** on duration of activity remains to be evaluated in longer duration experiments.

To evaluate potential interactions of a 2′-*O*-NMA substituent at the 5′-terminal of antisense strand moiety bound to the MID domain of Ago2, we turned to a crystal structure of an A-form duplex bearing 2′-*O*-NMA-T.[40] The structure allowed observation of six individual conformations of the NMA substituent, whereby the modified thymidine adopts a C3′-*endo* sugar pucker (Figure 5A). Conversely, in structures of RNA:Ago2
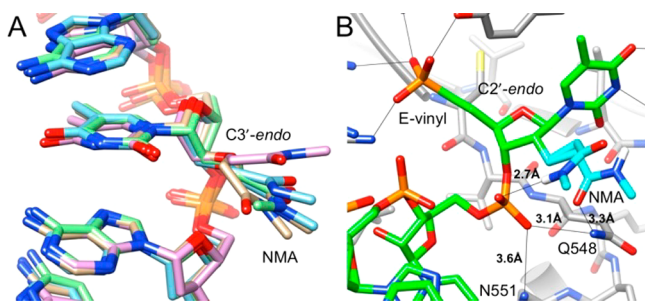
Figure 5. NMA conformation and interactions with the Ago2 MID domain. (A) Overlay of four strands from two A-form duplexes containing a single 2′-*O*-NMA-T per strand (PDB code 1XUX).[40] In one duplex 2′-*O*-NMA substituent of thymidine adopts two alternative conformations; the image thus depicts six NMA substituents. Strands were overlaid by superimposing modified thymidines together with 5′- and 3′-adjacent residues. (B) Putative interactions by the NMA substituent of the 5′-terminal antisense strand 5′-(*E*)-VP$_{NMA}$-T lodged in the Ago2 MID domain. Selected RNA:MID contacts are indicated by thin solid lines. Models are based on crystal structures of complexes between 5′-(*E*)-VP-modified RNA and human Ago2 (PDB code 5T7B,[6] PDB code 5JS2[5]). In one orientation, the NMA amido nitrogen is at ∼3.7 Å from the first bridging phosphate of the antisense strand, and in the alternative orientation, the NMA carbonyl oxygen forms a H-bond (distance of 3.3 Å) with the side chain of Q548. In the crystal structure of the NMA-modified duplex (A), the orientation with the NMA carbonyl group facing away from the nucleobase (four observations) is more common than the one with the carbonyl pointing to the same side as the base (two observations). Illustrations were generated with the program UCSF Chimera.[41]

complexes, the 5′-terminal nucleotide exhibits a DNA-like C2′-*endo* or C1′-*exo* pucker (see, for examples, Elkayam et al.[25] and Schirle et al.[24]). NMA-Ts from the duplex structure were superimposed on 5′-(*E*)-VP-T in the crystal structure of the Ago2 complex using only ribose C3′, C2′, and O2′ atoms to account for the different puckers of the nucleotides. Of the six resulting orientations of substituents two were selected to illustrate possibly stabilizing interactions between NMA atoms and the antisense strand and/or Ago2 residues (Figure 5B). In one orientation, less common judging from NMA conformations in the duplex crystal structure, the NMA amido group sits at ∼3.7 Å from OP2 of the first bridging phosphate of the antisense-strand RNA. In the second, more favorable orientation, the NMA carbonyl oxygen forms an H-bond to N*ε*2 of glutamine 548 that also interacts with the aforementioned phosphate together with asparagine 551 (Figure 5B). These structural considerations are consistent with the favorable in vitro and in vivo activity seen with 5′-(*E*)-VP$_{NMA}$-modified siRNAs.

■ CONCLUSION

In summary, we have established a simpler and more efficient protecting group strategy for incorporating the vinylphospho-

nate moiety at the 5′ end of oligonucleotides, which is based on the use of 5′-bis(POM)-protected phosphonate 3′-phosphoramidites. The strategy is compatible with standard oligonucleotide synthesis and deprotection conditions, therefore enhancing the scalability and scope of oligonucleotides containing a phosphonate moiety. 5′-(*E*)-VP-modified GalNAc-siRNA conjugates showed superior in vitro and in vivo RNAi activity as compared to their parent conjugates, whereas 5′-(*Z*)-VP was a poor phosphate mimic for siRNAs. We have also demonstrated that a nonphosphorylated nucleotide with moderately bulky 2′-*O*-NMA modification at the 5′-terminal of the antisense strand abolishes RNAi-mediated gene silencing. However, combining the 2′-*O*-NMA-modified nucleotide with a 5′-(*E*)-VP moiety rescued the in vivo activity and enhanced the duration of gene silencing, indicating that poor endogenous phosphorylation was predominantly responsible for the loss of activity observed for the parent 2′-*O*-NMA siRNA.

■ EXPERIMENTAL SECTION

Commercially available starting materials, reagents, and solvents were used as received. Anhydrous reactions were performed under an inert argon atmosphere. All monomeric compounds reported in this work were assessed for purity using NMR and or high performance liquid chromatography (HPLC) and were shown to be >95% purity except the intermediate aldehydes **5** and **6** and the mixture of compounds **9** and **11** and compounds **10** and **12**. The identities and purities of all oligonucleotides were confirmed using electrospray ionization mass spectrometry (ESI-MS) and ion-exchange HPLC (IEX-HPLC), respectively. The analytical purity and mass integrity of sense and antisense strands of siRNAs reported were determined by electrospray ionization LC−MS analysis; the observed masses were found to be within allowed ±2 range of the calculated mass.

Preparation of 3′-*O*-[(1,1-Dimethylethyl)dimethylsilyl]-2′-*O*-methyluridine 5. The reported compound **5** was synthesized from compound **3** according to literature procedures, and integrity and purity were confirmed by ¹H NMR analysis.[42]

Preparation of 5-Methyl-3′-*O*-[(1,1-dimethylethyl)-dimethylsilyl]-2′-*O*-[2-(methylamino)-2-oxoethyl]uridine 6. Compound **6** was synthesized from compound **4** by following literature procedure.[33] ¹H NMR (500 MHz, DMSO-d_6): δ 7.74 (d, J = 1.5 Hz, 1H), 7.42 (q, J = 5.2, 4.8 Hz, 1H), 5.83 (d, J = 4.4 Hz, 1H), 4.31 (t, J = 5.0 Hz, 1H), 4.07 (t, J = 4.6 Hz, 1H), 3.96 (s, 2H), 3.89 (dt, J = 5.6, 3.2 Hz, 1H), 3.69 (dd, J = 12.2, 3.3 Hz, 1H), 3.53 (dd, J = 12.1, 3.1 Hz, 1H), 1.97 (s, 1H), 1.75 (d, J = 1.1 Hz, 3H), 0.86 (s, 10H), 0.08 (d, J = 8.3 Hz, 6H). ¹³C NMR (126 MHz, DMSO-d_6): δ 170.3, 168.8, 164.0, 150.8, 136.0, 109.1, 86.5, 84.5, 81.0, 69.5, 69.2, 59.7, 60.0, 40.0, 39.92, 39.83, 39.75, 39.7, 39.6, 39.5, 39.3, 39.2, 39.0, 25.8, 25.63, 25.57, 25.2, 20.7, 17.7, 14.1, 12.3, −4.9, −5.1. HRMS: [M + Na]⁺ calcd for $C_{19}H_{33}N_3NaO_7Si$, 466.2100; found, 466.1993.

Preparation of 5′-Deoxy-3′-*O*-[(1,1-dimethylethyl)dimethyl-silyl]-2′-*O*-methyl-5′-oxouridine 7. To an ice cold solution of compound **5** (3.0 g, 8 mmol) in 150 mL of anhydrous dichloromethane was added Dess−Martin periodinane (4.7 g, 11.2 mmol, 1.4 mol equiv). The reaction mixture was stirred at 0 °C for 1 h and then at room temperature for 3 h. TLC analysis (eluent, ethyl acetate/hexane 7:3, v/v) confirmed formation of the product. The reaction mixture was then added to a 200 mL solution of 10% $Na_2S_2O_3$ and saturated $NaHCO_3$ (1:1), followed by addition of 200 mL ethyl acetate. The crude aldehyde was extracted into ethyl acetate dried over anhydrous Na_2SO_4 and concentrated under reduced pressure. The crude aldehyde **7** (2.87 g) thus obtained could be used without further purification. LC−MS of compound **7**: *m/z* 371.

Preparation of 5-Methyl-5′-deoxy-3′-*O*-[(1,1-Dimethylethyl)dimethylsilyl]-2′-*O*-[2-(methylamino)-2-oxoeth-yl]-5′-oxouridine 8. Compound **8** (20 g, yield 68%) was synthesized from compound **6** (32g, 72 mmol) and Dess−Martin periodinane (42 g, 101 mmol) as described above for the preparation of the aldehyde **7**.

The crude aldehyde thus obtained could be used without further purification. LC−MS of compound **8**: m/z 442.

Preparation of Mixture of Compounds 9 and 11. Tetrakis-[(pivaloyloxy)methyl] methylenediphosphonate[34] (**20**, 12.6 g, 20 mmol) was added into a stirring suspension of sodium hydride (0.58 g, 24 mmol) in 14 mL of anhydrous THF at −78 °C under argon atmosphere, and the stirring was continued for 15 min. A solution of the aldehyde **7** (2.86 g) in 40 mL of anhydrous THF was added dropwise to the mixture in THF, stirring at −78 °C. After completion of the addition, the reaction mixture was stirred successively for 1 h at −78 and 0 °C and at room temperature. TLC analysis confirmed formation of the product (eluent, ethyl acetate/hexanes 7:3, v/v). The crude reaction mixture was poured into 300 mL of saturated ammonium chloride solution, and the product was extracted into ethyl acetate (300 mL). The organic layer was washed with brine, dried over anhydrous Na_2SO_4. The solution was then concentrated under reduced pressure, and the residue was purified by flash silica gel column chromatography (eluent, ethyl acetate/hexanes 20−100%, v/v) to give compounds **9** and **11** (4.0 g) as a 9:1 mixture of E- and Z-isomers in 72% combined yield. Attempts to separate the mixture were not successful. ^{31}P NMR (162 MHz, $CDCl_3$) of the mixture: δ 14.5, 16.9.

Preparation of Mixture of Compounds 10 and 12. The mixture of E- and Z-isomers **10** and **12** (24 g, combined yield of 69%) was prepared from compound **8** (20 g, 45 mmol), (tetrakis-[(pivaloyloxy)methyl] methylenediphosphonate[34] (**20**), and sodium hydride as described above for the preparation of the a mixture of compounds **9** and **11**. ^{31}P NMR (202 MHz, CD_3CN) of the mixture: δ 15.2, 17.5.

Preparation of Compounds 13 and 15. A solution containing mixture of compounds **9** and **11** (4 g, 5.7 mmol) in 200 mL of $HCOOH/H_2O$ (1:1, v/v) was stirred at room temperature for 24 h. TLC analysis confirmed formation of the product (eluent, methanol/CH_2Cl_2 5:95 v/v). The solution was concentrated under reduced pressure, and the residue was purified by silica gel column chromatography (eluent, methanol/CH_2Cl_2 7:93, v/v). Fractions were tested on RP-HPLC (C18 column, buffer A = 0.05% trifluoroacetic acid in water, buffer B = 0.05% trifluoroacetic acid in acetonitrile; gradient 5−95% over 25 min) to confirm the purity of the E- and Z-isomers isolated. The E- and Z-isomers elute at 14.1 and 14.9 min, respectively (Supporting Information, Figures S18 and S19). Initial fractions from silica gel chromatography were mixtures of both isomers, whereas the later fractions contained only the E-isomer. The fractions containing both E- and Z-isomers were pooled, concentrated, and then the isomers were separated on RP-HPLC. Isolated yield: E-isomer **13** (23 g, 68%) and Z-isomer (0.3 g, 10%).

E-Isomer 13. ^1H NMR (500 MHz, DMSO-d_6): δ 11.44−11.39 (s, 1H), 7.63 (d, J = 8.0 Hz, 1H), 6.82 (t, J = 5.9 Hz, 1H), 6.16−6.01 (m, 1H), 5.81 (d, J = 4.3 Hz, 1H), 5.67−5.57 (m, 5H), 4.38−4.31 (m, 1H), 4.10 (t, J = 5.7 Hz, 1H), 3.94 (t, J = 4.8 Hz, 1H), 3.37 (s, 3H), 1.14 (s, 18H). ^{13}C NMR (126 MHz, DMSO-d_6): δ 176.0, 162.9, 150.3, 141.2, 102.2, 88.1, 81.6, 81.51, 81.47, 81.1, 57.8, 72.1, 38.2, 26.4. ^{31}P NMR (162 MHz, DMSO-d_6): δ 18.14. HRMS: $[M + Na]^+$ calcd for $C_{23}H_{35}N_2NaO_{12}P$, 585.1825; found, 585.1836.

Z-Isomer 15. ^1H NMR (500 MHz, DMSO-d_6): δ 11.39 (s, 1H), 7.71 (d, J = 8.1 Hz, 1H), 6.80 (m, 1H), 5.99−5.92 (m, 1H), 5.83 (d, J = 5.1 Hz, 1H), 5.61 (m, 5H), 5.36 (s, 1H), 5.13 (m, 1H), 4.06 (s, 1H), 3.99 (t, J = 5.1 Hz, 1H), 3.44−3.36 (m, 3H), 1.15 (s, 18H). ^{13}C NMR (126 MHz, DMSO-d_6): δ 176.0, 175.9, 162.9, 150.4, 150.3, 141.2, 102.2, 87.4, 81.44, 81.42, 81.40, 81.38, 81.36, 79.8, 79.7, 72.57, 72.55, 57.6, 38.2, 26.44, 26.42. ^{31}P NMR (202 MHz, DMSO-d_6): δ 15.85. HRMS: $[M + Na]^+$ calcd for $C_{23}H_{35}N_2NaO_{12}P$, 585.1825; found, 585.1818.

Preparation of Compounds 14 and 16. Compounds **14** and **16** were synthesized and isolated from the mixture of **10** and **12** using a procedure similar to that used to prepare compounds **11** and **15**.

E-Isomer 14. ^1H NMR (500 MHz, DMSO-d_6): δ 11.40 (s, 1H), 7.83 (q, J = 5.1, 4.6 Hz, 1H), 7.41 (s, 1H), 6.86−6.76 (m, 1H), 6.09 (m, 1H), 5.83 (d, J = 2.6 Hz, 1H), 5.62−5.59 (m, 4H), 4.36 (t, J = 5.8 Hz, 1H), 4.16−4.12 (m, 2H), 4.02 (d, J = 4.8 Hz, 2H), 2.49 (p, J = 1.8

Hz, 2H), 1.77 (s, 3H), 1.13 (s, 19H). ^{13}C NMR (126 MHz, DMSO-d_6): δ 176.0, 169.1, 168.1, 163.7, 162.2, 150.3, 149.4, 149.4, 140.5, 138.8, 136.7, 132.4, 130.0, 128.1, 118.5, 117.0, 109.8, 109.5, 109.1, 94.0, 88.7, 82.0, 81.8, 81.54, 81.49, 80.8, 80.7, 72.4, 69.4, 69.3, 40.1, 39.0, 38.3, 38.2, 26.6, 26.4, 26.3, 25.1, 22.3, 12.6, 12.0. ^{31}P NMR (202 MHz, DMSO-d_6): δ 17.05. HRMS: $[M + Na]^+$ calcd for $C_{26}H_{40}N_3NaO_{13}P$, 656.2196; found, 656.2194.

Z-Isomer 16. ^1H NMR (500 MHz, DMSO-d_6): δ 11.38 (s, 1H), 7.84 (q, J = 4.7 Hz, 1H), 7.49 (d, J = 1.5 Hz, 1H), 6.75 (m, 1H), 5.98 (m, 1H), 5.83 (d, J = 4.4 Hz, 1H), 5.62−5.57 (m, 5H), 5.13 (dd, J = 9.4, 5.5 Hz, 1H), 4.19 (t, J = 4.9 Hz, 1H), 4.09 (q, J = 5.7 Hz, 1H), 4.00 (d, J = 5.7 Hz, 2H), 2.49 (p, J = 1.8 Hz, 3H), 1.78 (s, 3H), 1.14 (d, J = 13.0 Hz, 19H). ^{13}C NMR (126 MHz, DMSO-d_6): δ 176.00, 175.95, 169.1, 163.7, 150.4, 150.1, 150.0, 136.6, 109.8, 88.0, 81.45, 81.41, 81.38, 81.0, 79.0, 78.9, 72.9, 69.4, 38.19, 38.17, 26.4, 26.4, 25.1, 12.0. ^{31}P NMR (202 MHz, DMSO-d_6): δ 14.70. HRMS: $[M + Na]^+$ calcd for $C_{26}H_{40}N_3NaO_{13}P$, 656.2196; found, 656.2187.

Preparation of Compound 17. To a solution of compound **13** (2.1 g, 3.62 mmol) and 5-(ethylthio)-1H-tetrazole (0.46 g, 3.62 mmol) in anhydrous acetonitrile (40 mL) was added 2-cyanoethyl N,N,N',N'-tetraisopropylphosphordiamidite (1.31 g, 4.35 mmol). The reaction mixture was stirred at room temperature for 2 h. TLC analysis in ethyl acetate/hexanes (2:8, v/v) containing 0.15% triethylamine confirmed formation of the product. The reaction mixture was filtered, concentrated, and loaded onto a silica column. The sample was eluted with 20−100% ethyl acetate in hexanes containing 0.15% triethylamine to afford compound **17** as a white foam (1.75 g, 62%). ^1H NMR (400 MHz, CD_3CN): δ 9.09 (s, 1H), 7.38 (d, J = 8.1 Hz, 1H), 6.89 (m, 1H), 6.10 (m, 1H), 5.86 (t, J = 3.8 Hz, 1H), 5.67−5.55 (m, 5H), 4.66−4.50 (m, 1H), 4.40−4.20 (m, 1H), 3.99 (m, 1H), 3.92−3.57 (m, 4H), 3.44 (s, 3H), 2.73−2.64 (m, 2H), 2.14 (s, 1H), 1.24−1.14 (m, 30H); ^{31}P NMR (162 MHz, CD_3CN): δ 152.02, 151.58, 18.23, 17.89.

Preparation of Compounds 18 and 19. Compounds **18** (7 g, 64%) and **19** (0.3 g, 65%) were prepared from compounds **14** (8 g, 13 mmol) and **15** (0.35 g, 0.604 mmol), respectively and 5-(ethylthio)-1H-tetrazole as described for the synthesis of the phosphoramidite **17**.

Compound 18. ^1H NMR (400 MHz, CD_3CN): δ = 9.27−9.03 (s, 1H), 7.22−7.16 (d, J = 1.4 Hz, 1H), 7.06−6.79 (m, 2H), 6.20−6.03 (m, 1H), 5.94−5.83 (dd, J = 3.5, 2.3 Hz, 1H), 5.69−5.56 (m, 4H), 4.70−4.55 (m, 1H), 4.42−4.26 (m, 1H), 4.25−4.01 (m, 3H), 3.95−3.82 (m, 1H), 3.80−3.70 (m, 1H), 3.80−3.70 (m, 1H), 3.69−3.55 (m, 2H), 2.82−2.60 (m, 5H), 1.90−1.76 (m, 3H), 1.35−1.03 (d, J = 4.7, 30H). ^{31}P NMR (162 MHz, CD_3CN): δ 152.09, 151.22, 18.44, 17.92.

Compound 19. ^1H NMR (400 MHz, CD_3CN): δ 9.02 (s, 1H), 7.41 (dd, J = 8.1, 1.6 Hz, 1H), 6.62 (m, 1H), 5.97 (dd, J = 17.4, 13.1 Hz, 1H), 5.80 (dd, J = 7.0, 3.5 Hz, 1H), 5.70−5.52 (m, 5H), 5.41 (m, 1H), 4.40−4.10 (m, 1H), 4.06−3.98 (m, 1H), 3.93−3.56 (m, 4H), 3.47 (s, 3H), 2.68 (m, 2H), 2.14 (s, 1H), 1.33−1.11 (m, 30H); ^{31}P NMR (202 MHz, CD_3CN): δ 151.16, 150.46, 15.17.

Synthesis of Oligonucleotides. Oligonucleotide synthesis was performed on a DNA/RNA synthesizer at scales between 1−10 μmol using commercially available 5′-O-(4,4′-dimethoxytrityl)-2′-deoxy-2′-fluoro- and 5′-O-(4,4′-dimethoxytrityl)-2′-O-methyl-3′-O-(2-cyanoethyl-N,N-diisopropyl) phosphoramidite monomers of uridine, 4-N-acetylcytidine, 6-N-benzoyladenosine, and 2-N-isobutyrylguanosine using standard solid-phase oligonucleotide synthesis protocols.[37,43] The GalNAc ligand was introduced at the 3′ end of the sense strand of the siRNA using a functionalized solid support as described.[12] The (n − 1)-mer of the desired antisense strand was first synthesized on a solid-support under standard solid-phase synthesis conditions. The VP-modified phosphoramidites **17**, **18**, and **19** were then individually introduced at the 5′-terminal of the solid-support bound and 5′-DMTr-deprotected (n − 1)-mer oligonucleotide under similar conditions using 0.25 M 5-(ethylthio)-1H-tetrazole in acetonitrile as phosphoramidite activator to obtain the desired 5′-phosphonate-modified full length antisense strand. Standard thiolation protocols with either 3-[(dimethylaminomethylene)amino]-3H-1,2,4-dithiazole-5-thione[44] or phenylacetyl disulfide[45] were performed to convert the phosphite triester into a phosphorothioate linkage. Since the

vinylphosphonate building blocks lack a DMTr-protecting group at the 5′-position, the final detritylation step was omitted. After completion of synthesis, the 5′-phosphonate-modified oligonucleotides were deprotected in 40% methylamine solution w/v for 15 min at 65 °C.

The crude oligonucleotides were purified by IEX-HPLC using column packed with TSK-Gel Super Q-5PW support and a linear gradient of 22−42% buffer B over 130 min with 50 mL/min flow rate (buffer A of 0.02 M Na_2HPO_4 in 10% acetonitrile, pH 8.5, and buffer B of buffer A plus 1 M NaBr). All single strands were purified to >80% HPLC (260 nm) purity and then desalted by size exclusion chromatography on an AKTA Prime chromatography system using an AP-2 glass column (20 mm × 300 mm) custom-packed with Sephadex G25, eluted with sterile nuclease-free water. The isolated yields for the final oligonucleotides were calculated based on the respective ratios of measured to theoretical 260 nm optical density units. The purified oligonucleotides were subjected to analytical ESI LC−MS and IEX-HPLC to determine mass and final purity (Supporting Information, Table S1). Equimolar amounts of complementary sense and antisense strands were mixed and annealed by heating in a water bath at 95 °C for 5 min and cooling to room temperature to obtain the desired siRNAs. The siRNA samples were analyzed for purity, endotoxin, and osmolality, and the observed values were within the allowed range for the concentration tested.

In Vitro Gene Silencing Experiments. Transfection experiments: 7.4 μL of Opti-MEM and 0.1 μL of Lipofectamine RNAiMax (Invitrogen) were added to 2.5 μL of conjugates per well into a 384-well plate and incubated at room temperature for 15 min. An amount of 40 μL of William's E medium (Life Technologies) containing ∼5 × 10^3 primary mouse hepatocytes cells was then added to the siRNA mixture. Cells were incubated for 24 h prior to RNA purification. mRNA was isolated with an automated BioTek-EL406 using Dynabeads mRNA DIRECT kits (ThermoFisher), which was followed by cDNA synthesis using high capacity cDNA reverse transcription kits (Applied Biosystems). qPCR reactions were performed in 384-well plates (Roche) and included 2 μL of cDNA, 0.5 μL of mouse *GAPDH* TaqMan VIC probe (4352339E, ThermoFisher), and 0.5 μL mouse target FAM probe (*Ttr* Mm00443267_m1 and *ApoB* Mm01545150_m1, ThermoFisher) in a volume of 10 mL. Values are plotted as a fraction of untreated control cells, and data were normalized to cells transfected with a nontargeting control siRNA. Each sample was run in technical duplicate, and each point represents the mean of 2 biological samples ± % error. Dose−response experiments were done over a range of doses from 100 to 3 × 10^{-07} nM final duplex concentration. *Gapdh* served as the internal control. IC_{50} values and dose−response curves (Figure S1) were generated using XLFit software.

In Vivo Gene Silencing Experiments. All procedures using mice were conducted by certified laboratory personnel using protocols consistent with local, state, and federal regulations, as applicable, and approved by the (i) Institutional Animal Care and Use Committee and (ii) AAALAC (Association for Assessment and Accreditation of Laboratory Animal Care International), accreditation number 001345. C57BL/6 female mice, aged 6−8 weeks acquired from Charles River Laboratories (*n* = 3 per group), were dosed subcutaneously at a volume of 10 μL of conjugate per gram of body weight. Control group was dosed with phosphate buffered saline (PBS). Serum samples were collected and LDL levels were analyzed for *ApoB* conjugates using the ADVIA 120 Hematology Systems from Siemens. Serum samples were collected from animals dosed with conjugates **2**, **2_NMA**, **2E-VP**, and **2E-VP_NMA** predose as well as 3, 7, 14, and 21 days postdose. Group averages are depicted with standard error. Individual animal data are provided in Figure S3.

Quantification of Whole Liver and Ago2-Associated siRNA Levels. Mice were dosed with either 1 mg/kg siRNA targeting *Ttr* (**1**, **1E-VP**, **1Z-VP**) or 10 mg/kg siRNA targeting *ApoB* (**2**, **2E-VP**, **2Z-VP**) and were sacrificed on day 7 postdose. Livers were snap frozen in liquid nitrogen and ground into powder for further analysis. Total siRNA liver levels were measured by reconstituting liver powder at 10 mg/mL in PBS containing 0.25% Triton-X 100. The tissue suspension was further ground with 5-mm steel grinding balls (Qiagen) at 50

cycles/s for 5 min in a tissue homogenizer (Qiagen TissueLyser LT) at 4 °C. Homogenized samples were then heated at 95 °C for 5 min, briefly vortexed, and allowed to rest on ice for 5 min. Samples were then centrifuged at 21 000g for 5 min at 4 °C. The siRNA-containing supernatants were transferred to new tubes. siRNA sense and antisense strand levels were quantified by stem loop reverse transcription followed by Taqman PCR (SL-RT QPCR) based on previously published methods.[46,47] Primers used for SL-RT QPCR are summarized in Supporting Information Table S2.

Ago2-bound siRNA was quantified by preparing liver powder lysates at 100 mg/mL in lysis buffer (50 mM Tris-HCl, pH 7.5, 150 mM NaCl, 2 mM EDTA, 0.5% Triton-X 100) supplemented with freshly added protease inhibitors (Sigma-Aldrich, P8340) at 1:100 dilution and PMSF (1 mM final concentration, Life Technologies). Total liver lysate (10 mg) was used for each Ago2 immunoprecipitation (IP) and control IP. Anti-Ago2 antibody was purchased from Wako Chemicals (clone no. 2D4). Control mouse IgG was from Santa Cruz Biotechnology (sc-2025). Protein G Dynabeads (Life Technologies) were used to precipitate antibodies. Ago2-associated siRNAs were eluted by heating (50 μL of PBS, 0.25% Triton; 95 °C, 5 min) and measured by SL-RT QPCR. Primers used for SL-RT QPCR are summarized in Table S2.

ASSOCIATED CONTENT

Ⓢ Supporting Information

AUTHOR INFORMATION

Corresponding Authors

*M.M.: e-mail, mmanoharan@alnylam.com.

*K.G.R.: e-mail, rajeevk@alnylam.com.

ORCID Ⓘ

Kallanthottathil G. Rajeev: 0000-0002-0104-0237

Notes

ACKNOWLEDGMENTS

ABBREVIATIONS USED

Ago2, Argonaute 2; ASGPR, asialoglycoprotein receptor; *Apo B*, apolipoprotein B; ESI-MS, electrospray ionization mass spectrometry; GalNAc, *N*-acetylgalactosamine; hATTR, hereditary ATTR; IEX-HPLC, ion exchange high-performance liquid chromatography; LC−MS, liquid chromatography−mass spectrometry; POM, pivaloyloxymethyl; RISC, RNA-induced silencing complex; RNAi, RNA interference; siRNA, small interfering RNA; GalNAc-siRNA, *N*-acetylgalactosamine conjugated siRNA; SL-RT QPCR, stem loop real-time quantitative polymerase chain reaction; *Ttr*, transthyretin; VP, vinylphosphonate

■ REFERENCES

(1) Manoharan, M. RNA interference and chemically modified small interfering RNAs. *Curr. Opin. Chem. Biol.* **2004**, *8*, 570−579.

(2) Bumcrot, D.; Manoharan, M.; Koteliansky, V.; Sah, D. W. Y. RNAi therapeutics: a potential new class of pharmaceutical drugs. *Nat. Chem. Biol.* **2006**, *2*, 711−719.

(3) Manoharan, M.; Rajeev, K. G. Utilizing chemistry to harness RNA interference pathways for therapeutics: chemically modified siRNAs and antagomirs. *Antisense Drug Technology: Principles, Strategies, and Applications*, 2nd ed.; CRC Press: Boca Raton, FL, 2008; pp 437−464.

(4) Wittrup, A.; Lieberman, J. Knocking down disease: a progress report on siRNA therapeutics. *Nat. Rev. Genet.* **2015**, *16*, 543−552.

(5) Titze-de-Almeida, R.; David, C.; Titze-de-Almeida, S. S. The Race of 10 Synthetic RNAi-based drugs to the pharmaceutical market. *Pharm. Res.* **2017**, *34*, 1339−1363.

(6) Tam, C.; Wong, J. H.; Cheung, R. C. F.; Zuo, T.; Ng, T. B. Therapeutic potentials of short interfering RNAs. *Appl. Microbiol. Biotechnol.* **2017**, *101*, 7091−7111.

(7) Adams, D.; Suhr, O. B.; Dyck, P. J.; Litchy, W. J.; Leahy, R. G.; Chen, J.; Gollob, J.; Coelho, T. Trial design and rationale for APOLLO, a Phase 3, placebo-controlled study of patisiran in patients with hereditary ATTR amyloidosis with polyneuropathy. *BMC Neurol.* **2017**, *17*, 181.

(8) Butler, J. S.; Chan, A.; Costelha, S.; Fishman, S.; Willoughby, J. L. S.; Borland, T. D.; Milstein, S.; Foster, D. J.; Goncalves, P.; Chen, Q.; Qin, J.; Bettencourt, B. R.; Sah, D. W.; Alvarez, R.; Rajeev, K. G.; Manoharan, M.; Fitzgerald, K.; Meyers, R. E.; Nochur, S. V.; Saraiva, M. J.; Zimmermann, T. S. Preclinical evaluation of RNAi as a treatment for transthyretin-mediated amyloidosis. *Amyloid* **2016**, *23*, 109−118.

(9) Jono, H.; Ando, Y. Towards targets and treatments in transthyretin amyloidosis. *Expert Opin. Orphan Drugs* **2017**, *5*, 691−699.

(10) Adams, D.; Gonzalez-Duarte, A.; O'Riordan, W.; Yang, C. C.; Yamashita, T.; Kristen, A.; Tournev, I.; Schmidt, H.; Coelho, T.; Berk, J.; Lin, K. P.; Sweetser, M.; Gandhi, P.; Chen, J.; Gollob, J.; Suhr, O. B. Patisiran, an investigational RNAi therapeutic for the treatment of hereditary ATTR amyloidosis with polyneuropathy: results from the phase 3 APOLLO study. EU ATTR Meeting, November 2, 2017, Paris; http://www.alnylam.com/wp-content/uploads/2017/11/EU-ATTR-2017_APOLLO-TRL_CAPELLA_FINAL_2Nov2017.pdf.

(11) Berk, J. L.; Adams, D.; Suhr, O.; Conceicao, I.; Cruz, M. W.; Schmidt, H.; Buades, J.; Campistol, J. M.; Pouget, J. Y.; Polydefkis, M.; Sweetser, M.; Partisano, A. M.; Chen, J.; Gollob, J.; Coelho, T. Long-term, open-label clinical experience with patisiran, an investigational RNAi therapeutic for patients with hereditary transthyretin-mediated (hATTR) amyloidosis with polyneuropathy. EU ATTR Meeting, November 2, 2017, Paris; http://www.alnylam.com/wp-content/uploads/2017/11/EU-ATTR_Ph2-OLE-36-month-Poster_RPD-FINAL.pdf.

(12) Nair, J. K.; Willoughby, J. L. S.; Chan, A.; Charisse, K.; Alam, M. R.; Wang, Q.; Hoekstra, M.; Kandasamy, P.; Kel'in, A. V.; Milstein, S.; Taneja, N.; O'Shea, J.; Shaikh, S.; Zhang, L.; van der Sluis, R. J.; Jung, M. E.; Akinc, A.; Hutabarat, R.; Kuchimanchi, S.; Fitzgerald, K.; Zimmermann, T.; van Berkel, T. J. C.; Maier, M. A.; Rajeev, K. G.; Manoharan, M. Multivalent *N*-acetylgalactosamine-conjugated siRNA localizes in hepatocytes and elicits robust RNAi-mediated gene silencing. *J. Am. Chem. Soc.* **2014**, *136*, 16958−16961.

(13) Spiess, M. The asialoglycoprotein receptor: a model for endocytic transport receptors. *Biochemistry* **1990**, *29*, 10009−10018.

(14) Grewal, P. K. The Ashwell-Morell receptor. *Methods Enzymol.* **2010**, *479*, 223−241.

(15) Huang, X.; Leroux, J. C.; Castagner, B. Well-defined multivalent ligands for hepatocytes targeting *via* asialoglycoprotein receptor. *Bioconjugate Chem.* **2017**, *28*, 283−295.

(16) Weitzer, S.; Martinez, J. The human RNA kinase hClp1 is active on 3′ transfer RNA exons and short interfering RNAs. *Nature* **2007**, *447*, 222−226.

(17) Kuhn, C.-D.; Joshua-Tor, L. Eukaryotic argonautes come into focus. *Trends Biochem. Sci.* **2013**, *38*, 263−271.

(18) Tolia, N. H.; Joshua-Tor, L. Slicer and the argonautes. *Nat. Chem. Biol.* **2007**, *3*, 36−43.

(19) Parmar, R.; Willoughby, J. L. S.; Liu, J.; Foster, D. J.; Brigham, B.; Theile, C. S.; Charisse, K.; Akinc, A.; Guidry, E.; Pei, Y.; Strapps, W.; Cancilla, M.; Stanton, M. G.; Rajeev, K. G.; Sepp-Lorenzino, L.; Manoharan, M.; Meyers, R.; Maier, M. A.; Jadhav, V. 5′-(*E*)-Vinylphosphonate: a stable phosphate mimic can improve the RNAi activity of siRNA-GalNAc conjugates. *ChemBioChem* **2016**, *17*, 985−989.

(20) Lima, W. F.; Prakash, T. P.; Murray, H. M.; Kinberger, G. A.; Li, W.; Chappell, A. E.; Li, C. S.; Murray, S. F.; Gaus, H.; Seth, P. P.; Swayze, E. E.; Crooke, S. T. Single-stranded siRNAs activate RNAi in animals. *Cell* **2012**, *150*, 883−894.

(21) Prakash, T. P.; Lima, W. F.; Murray, H. M.; Li, W.; Kinberger, G. A.; Chappell, A. E.; Gaus, H.; Seth, P. P.; Bhat, B.; Crooke, S. T.; Swayze, E. E. Identification of metabolically stable 5′-phosphate analogs that support single-stranded siRNA activity. *Nucleic Acids Res.* **2015**, *43*, 2993−3011.

(22) Chang, W.; Pei, Y.; Guidry, E. N.; Zewge, D.; Parish, C. A.; Sherer, E. C.; DiMuzio, J.; Zhang, H.; South, V. J.; Strapps, W. R.; Sepp-Lorenzino, L.; Colletti, S. L.; Stanton, M. G. Systematic chemical modifications of single stranded siRNAs significantly improved CTNNB1 mRNA silencing. *Bioorg. Med. Chem. Lett.* **2016**, *26*, 4513−4517.

(23) Haraszti, R. A.; Roux, L.; Coles, A. H.; Turanov, A. A.; Alterman, J. F.; Echeverria, D.; Godinho, B. M. D. C.; Aronin, N.; Khvorova, A. 5-Vinylphosphonate improves tissue accumulation and efficacy of conjugated siRNAs in vivo. *Nucleic Acids Res.* **2017**, *45*, 7581−7592.

(24) Schirle, N. T.; Kinberger, G. A.; Murray, H. F.; Lima, W. F.; Prakash, T. P.; MacRae, I. J. Structural analysis of human argonaute-2 bound to a modified siRNA guide. *J. Am. Chem. Soc.* **2016**, *138*, 8694−8697.

(25) Elkayam, E.; Joshua-Tor, L.; Parmar, R.; Brown, C. R.; Willoughby, J. L.; Theile, C. S.; Manoharan, M. siRNA carrying an (*E*)-vinylphosphonate moiety at the 5 end of the guide strand augments gene silencing by enhanced binding to human Argonaute-2. *Nucleic Acids Res.* **2017**, *45*, 3528−3536.

(26) Lavergne, T.; Bertrand, J.-R.; Vasseur, J.-J.; Debart, F. Base-labile group for 2′-OH protection of ribonucleosides: a major challenge for RNA synthesis. *Chem. - Eur. J.* **2008**, *14*, 9135−9138.

(27) Pradere, U.; Garnier-Amblard, E. C.; Coats, S. J.; Amblard, F.; Schinazi, R. F. Synthesis of nucleoside phosphate and phosphonate prodrugs. *Chem. Rev.* **2014**, *114*, 9154−9218.

(28) Vepsalainen, J. J. Bisphosphonate prodrugs. *Curr. Med. Chem.* **2002**, *9*, 1201−1208.

(29) Yu, R. Z.; Gunawan, R.; Post, N.; Zanardi, T.; Hall, S.; Burkey, J.; Kim, T.-W.; Graham, M. J.; Prakash, T. P.; Seth, P. P.; Swayze, E. E.; Geary, R. S.; Henry, S. P.; Wang, Y. Disposition and pharmacokinetics of a GalNAc3-conjugated antisense oligonucleotide targeting human lipoprotein (a) in monkeys. *Nucleic Acid Ther.* **2016**, *26*, 372−380.

(30) Tuschl, T. RNA interference and small interfering RNAs. *ChemBioChem* **2001**, *2*, 239−245.

(31) Hodge, R. P.; Sinha, N. D. Simplified synthesis of 2′-*O*-alkyl ribopyrimidines. *Tetrahedron Lett.* **1995**, *36*, 2933−2936.

(32) Prakash, T. P.; Kawasaki, A. M.; Wancewicz, E. V.; Shen, L.; Monia, B. P.; Ross, B. S.; Bhat, B.; Manoharan, M. Comparing in vitro and in vivo activity of 2′-*O*-[2-(methylamino)-2-oxoethyl]- and 2′-*O*-methoxyethyl-modified antisense oligonucleotides. *J. Med. Chem.* **2008**, *51*, 2766−2776.

(33) Kel'in, A. V.; Zlatev, I.; Harp, J.; Jayaraman, M.; Bisbe, A.; O'Shea, J.; Taneja, N.; Manoharan, R. M.; Khan, S.; Charisse, K.; Maier, M. A.; Egli, M.; Rajeev, K. G.; Manoharan, M. Structural basis of duplex thermodynamic stability and enhanced nuclease resistance of 5′-*C*-methyl pyrimidine-modified oligonucleotides. *J. Org. Chem.* **2016**, *81*, 2261−2279.

(34) Vepsalainen, J. J. Bisphosphonate prodrugs: a new synthetic strategy to tetraacyloxymethyl esters of methylenebisphosphonates. *Tetrahedron Lett.* **1999**, *40*, 8491−8493.

(35) Pradere, U.; Amblard, F.; Coats, S. J.; Schinazi, R. F. Synthesis of 5′-methylene-phosphonate furano-nucleoside prodrugs: application to D-2′-deoxy-2′-α-fluoro-2′-β-C-methyl nucleosides. *Org. Lett.* **2012**, *14*, 4426−4429.

(36) Sinha, N. D.; Biernat, J.; Koester, H. β-Cyanoethyl *N,N*-dialkylamino/N-morpholinomonochlorophosphoamidites, new phosphitylating agents facilitating ease of deprotection and work-up of synthesized oligonucleotides. *Tetrahedron Lett.* **1983**, *24*, 5843−5846.

(37) Damha, M. J.; Ogilvie, K. K. Oligoribonucleotide synthesis. The silyl-phosphoramidite method. *Methods Mol. Biol.* **1993**, *20*, 81−114.

(38) Zimmermann, T. S.; Lee, A. C. H.; Akinc, A.; Bramlage, B.; Bumcrot, D.; Fedoruk, M. N.; Harborth, J.; Heyes, J. A.; Jeffs, L. B.; John, M.; Judge, A. D.; Lam, K.; McClintock, K.; Nechev, L. V.; Palmer, L. R.; Racie, T.; Roehl, I.; Seiffert, S.; Shanmugam, S.; Sood, V.; Soutschek, J.; Toudjarska, I.; Wheat, A. J.; Yaworski, E.; Zedalis, W.; Koteliansky, V.; Manoharan, M.; Vornlocher, H.-P.; MacLachlan, I. RNAi-mediated gene silencing in non-human primates. *Nature* **2006**, *441*, 111−114.

(39) Prakash, T. P.; Kawasaki, A. M.; Lesnik, E. A.; Owens, S. R.; Manoharan, M. 2′-*O*-[2-(Amino)-2-oxoethyl] oligonucleotides. *Org. Lett.* **2003**, *5*, 403−406.

(40) Pattanayek, R.; Sethaphong, L.; Pan, C.; Prhavc, M.; Prakash, T. P.; Manoharan, M.; Egli, M. Structural rationalization of a large difference in RNA affinity despite a small difference in chemistry between two 2′-*O*-modified nucleic acid analogues. *J. Am. Chem. Soc.* **2004**, *126*, 15006−15007.

(41) Pettersen, E. F.; Goddard, T. D.; Huang, C. C.; Couch, G. S.; Greenblatt, D. M.; Meng, E. C.; Ferrin, T. E. UCSF Chimera-a visualization system for exploratory research and analysis. *J. Comput. Chem.* **2004**, *25*, 1605−1612.

(42) Prakash, T. P.; Kawasaki, A. M.; Lesnik, E. A.; Owens, S. R.; Manoharan, M. 2′-*O*-[2-(amino)-2-oxoethyl] oligonucleotides. *Org. Lett.* **2003**, *5*, 403−406.

(43) Beaucage, S. L. Solid-phase synthesis of siRNA oligonucleotides. *Curr. Opin. Drug Discovery Dev.* **2008**, *11*, 203−216.

(44) Guzaev, A. P. Reactivity of 3H-1,2,4-dithiazole-3-thiones and 3H-1,2-dithiole-3-thiones as sulfurizing agents for oligonucleotide synthesis. *Tetrahedron Lett.* **2011**, *52*, 434−437.

(45) Cheruvallath, Z. S.; Wheeler, P. D.; Cole, D. L.; Ravikumar, V. T. Use of phenylacetyl disulfide (PADS) in the synthesis of oligodeoxyribonucleotide phosphorothioates. *Nucleosides Nucleotides* **1999**, *18*, 485−492.

(46) Chen, C.; Ridzon, D. A.; Broomer, A. J.; Zhou, Z.; Lee, D. H.; Nguyen, J. T.; Barbisin, M.; Xu, N. L.; Mahuvakar, V. R.; Andersen, M. R.; Lao, K. Q.; Livak, K. J.; Guegler, K. J. Real-time quantification of microRNAs by stem-loop RT-PCR. *Nucleic Acids Res.* **2005**, *33*, e179.

(47) Cheng, A.; Li, M.; Liang, Y.; Wang, Y.; Wong, L.; Chen, C.; Vlassov, A. V.; Magdaleno, S. Stem-loop RT-PCR quantification of siRNAs in vitro and in vivo. *Oligonucleotides* **2009**, *19*, 203−208.